technologies

MDPI

Article

Comparing Elastocaloric Cooling and Desiccant Wheel Dehumidifiers for Atmospheric Water Harvesting

John LaRocco [1,*], Qudsia Tahmina [2], John Simonis [2] and Vidhaath Vedati [3]

[1] Department of Psychiatry and Behavioral Sciences, Wexner Medical Center, The Ohio State University, Columbus, OH 43210, USA
[2] Electrical and Computer Engineering, The Ohio State University, Columbus, OH 43210, USA; tahmina.1@osu.edu (Q.T.); simonis.15@osu.edu (J.S.)
[3] College of Arts and Sciences, The Ohio State University, Columbus, OH 43210, USA; vedati.2@osu.edu
* Correspondence: john.larocco@osumc.edu

Abstract: Approximately two billion people worldwide lack access to clean drinking water, negatively impacting national security, hygiene, and agriculture. Atmospheric water harvesting (AWH) is the conversion of ambient humidity into clean water; however, conventional dehumidification is energy-intensive. Improvement in AWH may be achieved with elastocaloric cooling, using temperature-sensitive materials in active thermoregulation. Potential benefits, compared to conventional desiccant wheel designs, include substantial reductions in energy use, size, and complexity. A nickel–titanium (NiTi) elastocaloric water harvester was designed and compared with a desiccant wheel design under controlled conditions of relative humidity, air volume, and power. In a 30 min interval, the NiTi device harvested more water on average at 0.18 ± 0.027 mL/WH, compared to the 0.1567 ± 0.023 mL/WH of the desiccant wheel harvester. Moreover, the NiTi harvester required half the power input and was thermoregulated more efficiently. Future work will focus on mechanical design parameter optimization. Elastocaloric cooling is a promising advancement in dehumidification, making AWH more economical and feasible.

Keywords: elastocaloric dehumidification; elastocaloric cooling; atmospheric water harvesting; desiccant wheel; dehumidification

Citation: LaRocco, J.; Tahmina, Q.; Simonis, J.; Vedati, V. Comparing Elastocaloric Cooling and Desiccant Wheel Dehumidifiers for Atmospheric Water Harvesting. *Technologies* **2024**, *12*, 178. https://doi.org/10.3390/technologies12100178

Received: 24 August 2024
Revised: 13 September 2024
Accepted: 26 September 2024
Published: 30 September 2024

1. Introduction

1.1. Overview

An estimated two billion people lack access to clean drinking water supplies, and water shortages can negatively impact national security, hygiene, and agriculture [1]. Although climate change has resulted in increased ambient humidity, traditional water sources are becoming increasingly depleted. Existing dehumidifiers can pull water from the air via atmospheric water harvesting (AWH), but they are large and energy-intensive [2]. Elastocaloric cooling and desiccant wheels are two technologies that may reduce the size, energy requirements, and cost of AWH [2]. Elastocaloric cooling is the use of temperature-sensitive materials in active thermoregulation, offering substantial reductions in energy use, size, and complexity. Desiccant wheels use hygroscopic materials to remove water molecules from airflow. An elastocaloric cooler and a desiccant wheel were fabricated and compared to identify the more efficient compact dehumidifier.

1.2. Background

1.2.1. Environment

Water is essential for human life. The average adult requires at least 4 L of water per day [3–5]. However, billions of people do not have access to sufficient supplies of clean water [1]. Economic and environmental pressures from climate change, population growth, and agriculture put strain on traditional water sources [6]. The lack of clean water has

greatly exacerbated existing issues in security, hygiene, food security, crime, wildfires, and even mental health [7–11]. While climate change has greatly increased atmospheric water vapor, exploiting this humidity requires specialized technology to pull water from the air [12]. AWH has been used since antiquity, but scaling it to provide even one person's needs requires a dehumidifier [13,14].

1.2.2. Dehumidifiers

Existing dehumidifiers are ill-suited for resource-scarce countries lacking modern infrastructure [2]. Current commercial machinery is bulky, energy-intensive, and slow. Passive methods, such as membranes, often require large air volumes and long timescales [13–15]. As many developing countries lack reliable electric power, the constant energy input needed by AWH makes it a costly option [16]. While solar-based solutions have been explored, they require long hours to generate even small amounts of water [17–19]. Even the latest, most efficient options require bulky equipment [2,17]. Thus, a portable, backpack-sized dehumidifier could resolve these issues; however, only a handful of technologies meet the essential requirements of portability, low cost, and energy efficiency [20–22].

1.2.3. Elastocaloric Cooling

Elastocaloric cooling uses temperature-sensitive materials for thermoregulation [23,24]. Shape-memory alloys change shape when exposed to specific temperatures and switch between discrete mechanical configurations [25–27]. The nickel–titanium alloy, also known as nitinol or NiTi, is the most commonly used material for elastocaloric cooling. Fatigue and wear on NiTi wire was an issue reported in prior work using wire bundles and tubes, which has greatly improved performance [28–31].

The wires change shape due to a molecular phase change when temperature causes a phase shift between austenite when cooled to martensite when heated [25–27]. During the martensite phase, the material's unit cell edge lengths are unequal and possess a slip angle of approximately 96°. In the austenite phase, the material's unit cell lengths are symmetrical and possess a slip angle of 90° [28–31].

Elastocaloric cooling systems have functioned by holding NiTi wires under tension, allowing them to reach thermal equilibrium with the local temperature [25–27]. Upon being released, the wires revert from martensite to austenite, allowing them to absorb ambient heat and cool their surroundings. As the wires reach thermal equilibrium, the phase change cools the immediate surroundings by absorbing ambient heat energy. The slight temperature change, when combined with a heatsink, can condense water [28–31].

Earlier elastocaloric cooling devices had applications ranging from computing to air conditioning and required a fifth of the energy and space of their conventional counterparts [32,33]. Elastocaloric cooling devices are being actively explored and refined, including their potential use as dehumidifiers [30,34]. However, they would have to compete with proven technology for moisture removal in heating, ventilation, and air conditioning (HVAC) [35,36].

1.2.4. Desiccant Wheels

Desiccant wheels are used to trap and remove humidity from airflow [20]; they are rotating cylinders lined with hydrophilic materials and commercially available desiccants, such as silica gel. Desiccant wheels are widely used in conventional HVAC. Their potential for AWH has been explored, often in the context of portable and energy-efficient designs [14]. However, the literature on small-scale designs is lacking [37], particularly regarding direct comparisons between other modalities [38].

2. Materials and Methods

2.1. Overview

Comparing elastocaloric cooling and desiccant wheel-based designs on a small scale permitted direct observation of their energy requirements and harvesting efficiency. Each prototype was tested in an environmental chamber at constant humidity and temperature. The energy consumption, heat generation, and water-harvesting efficiency were evaluated in test sessions of 30 min each. The performance of each device was automatically logged for comparison.

2.2. Experimental Designs

The experiment was conducted in a plastic storage container with a silicon sealing ring (Figure 1). To reduce the risk of rust, wires were tightly compressed by the lid, and electrical connections were sealed. A captive TR-1801 UCAREAIR ultrasonic humidifier, controlled from the outside, was fitted within the container (Kalorik Electronics Technology, Xiamen, China).

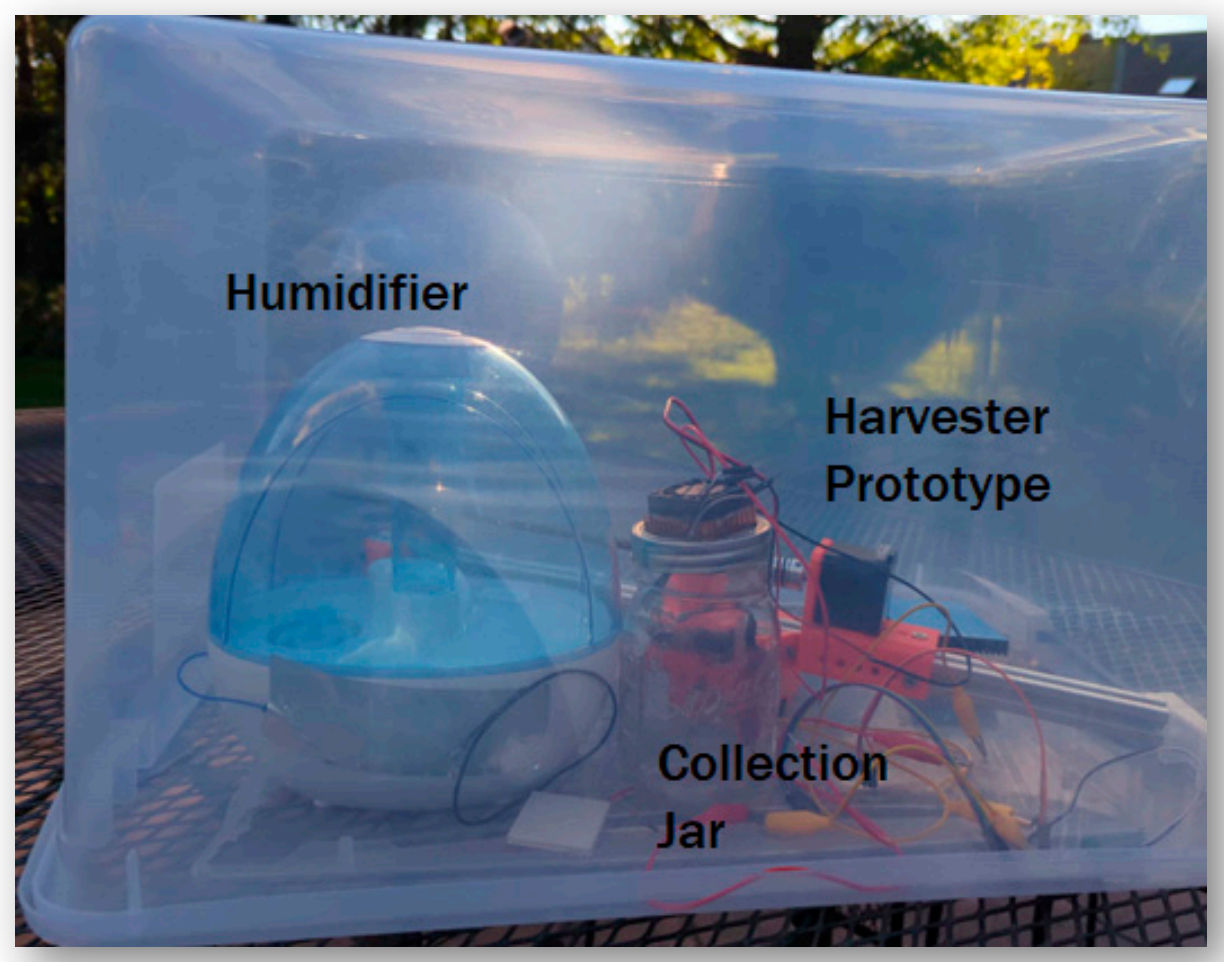

Figure 1. Experimental setup with labeled components.

A device used commercially in HVAC, namely the AHT20 I2C combined temperature and humidity sensor (Adafruit Industries, New York, NY, USA), was placed inside the container [36]. A small electric fan was used for air circulation. Power consumption was monitored using an ACS712 current sensor (Allegro, Worcester, MA, USA) and a steady direct current voltage of 24 V. The water level was monitored using a resistive rainfall sensor and a graduated cylinder. Data were streamed over a serial connection every 10 s to a PC.

2.3. Experimental Calculations

A dehumidifier's capability is rated by the volume of water removed from the air per hour; it is typically calculated using the room's area, temperature, relative humidity, and desired relative humidity [22]. Equation (1) is used to calculate dehumidification capacity D.

$$D = \frac{p * V * x}{n} \tag{1}$$

The volume of the container V was approximated at 1 m^3. An ambient temperature of 22 °C was used in the calculations based on the device's surroundings and baseline. The density of moist, humid air (p) was assumed to be constant at 1.2 $\frac{kg}{m^3}$ between 15 and 25 °C. The humidifier was set to generate a relative humidity x of 99.9%; the aim was to model "ideal" conditions for both dehumidifiers. The number of hours n was set to 30 min or 0.5 h. The water weight (W in kg) was converted to water volume (V_w in mL) using Equation (2).

$$V_w = W * 1000 \tag{2}$$

The total power was calculated from the drawn current over each experimental period [20]. The total power (P) was calculated using Equation (3). The voltage (V_{DC}) was a constant 24 V, and the current (I) was the average current over the experimental period.

$$P = V_{DC} * I \tag{3}$$

The total time and power, denoted in watt-hours (WH), was calculated using Equation (4).

$$WH = P * n \tag{4}$$

Adjusted for time, the total harvesting rate (R) per watt-hour was calculated using Equation (5), yielding the total harvest per watt.

$$R = \frac{D}{WH} \tag{5}$$

Using these calculations, the two water harvester designs were tested and compared for efficiency and yield [2,33].

$$R = \frac{1000 * \left(\frac{p*V*x}{n}\right)}{(V_{DC} * I * n)} \tag{6}$$

The observed harvesting rate is a function of the variables combined in Equation (6).

2.4. Model Designs

2.4.1. Desiccant Wheel Harvester

The desiccant wheel dehumidifier was used as the control design because of its widespread commercial use [38]. In the prototype, a temperature differential was used to generate condensation. A fan circulated air through the silica gel desiccant, and a generic ~150 W heat lamp was used to dry the pockets of desiccant. The desiccant wheel was mounted on a piece of wood and rotated while heated air was blown through each desiccant-filled rung on the wheel. The harvester comprised eight stacked rungs.

A heat lamp was positioned above the rotating desiccant wheel rings; the air was blown from the top, and a water basin was beneath them. The desiccant wheel rings were under constant heat from the lamp. Water vapor was forced out of the pockets into the basin, where a heatsink improved the condensation and connection. The components of the system are labeled in Figure 2.

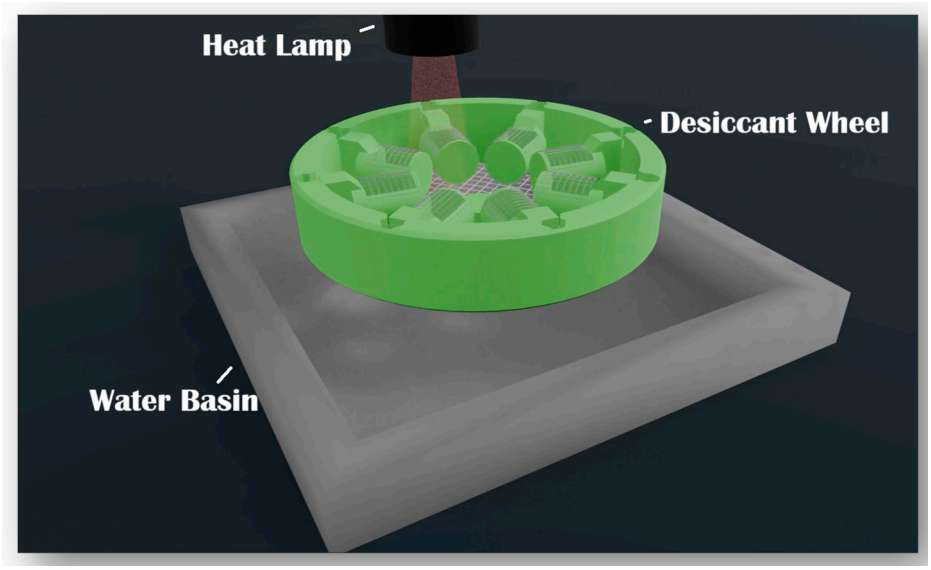

Figure 2. Desiccant wheel water harvester with components labeled.

Figure 3 displays the side and top views of a desiccant wheel rung.

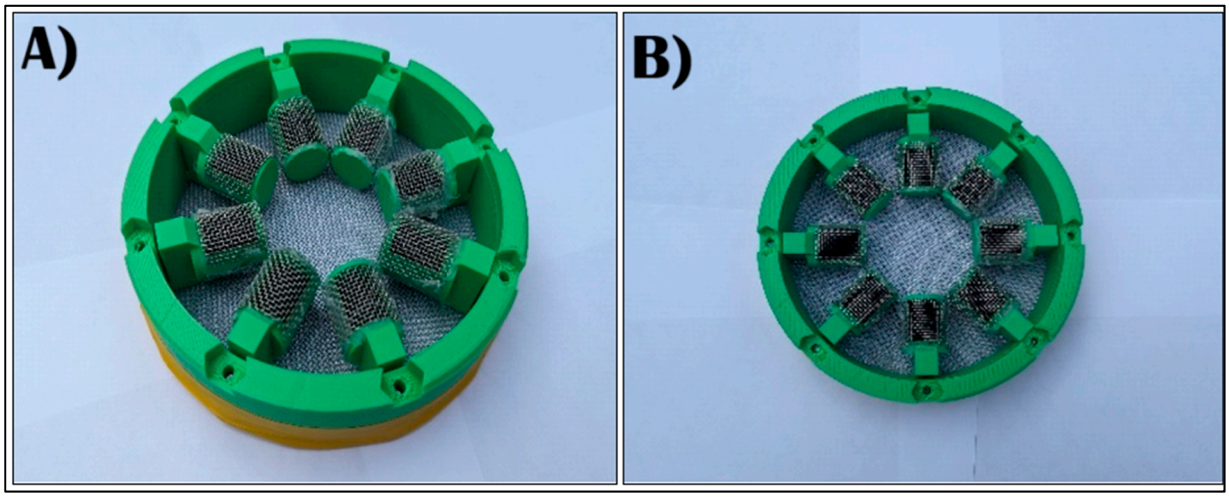

Figure 3. (**A**) Side view of a single rung of the desiccant wheel. (**B**) Top view of a single rung of the desiccant wheel.

Parts were designed using the SolidWorks 2024 3D software (Dassault Systèmes, Vélizy-Villacoublay, France) and then 3D printed in polyethylene terephthalate glycol (PETG), a durable thermoplastic polyester. The print was configured with one wheelbase and eight-wheel rungs. The print slicer settings were set to ensure 100% infill, with supports everywhere and a layer height of 0.16 mm or less. The rungs were each connected to the wheelbase and secured with M5 bolts and nuts.

2.4.2. NiTi Harvester

The NiTi water harvester had a straightforward gantry design, used in tandem with a high-torque Nema 17 stepper motor (OSM Technology, Ningbo, China) [28,29]. The elongated design and NiTi wires enabled it to collect water and regulate its temperature by moving the harvester to a different location. A T8 lead screw was used to apply more pressure to the NiTi wires, adding a slight mechanical advantage to the design. The NiTi harvester used 3D-printed components made by applying the same settings as those of the desiccant wheel harvester. The model was secured according to the prototype's rendering. Finally, T-nuts were fastened to the supplied gantry. The prototype was wired with a generic

8-A DC barrel jack power supply and controlled with an ATmega328P microcontroller (Microchip Technologies, Chandler, AZ, USA). Figure 4 shows the side and top views of the NiTi harvester.

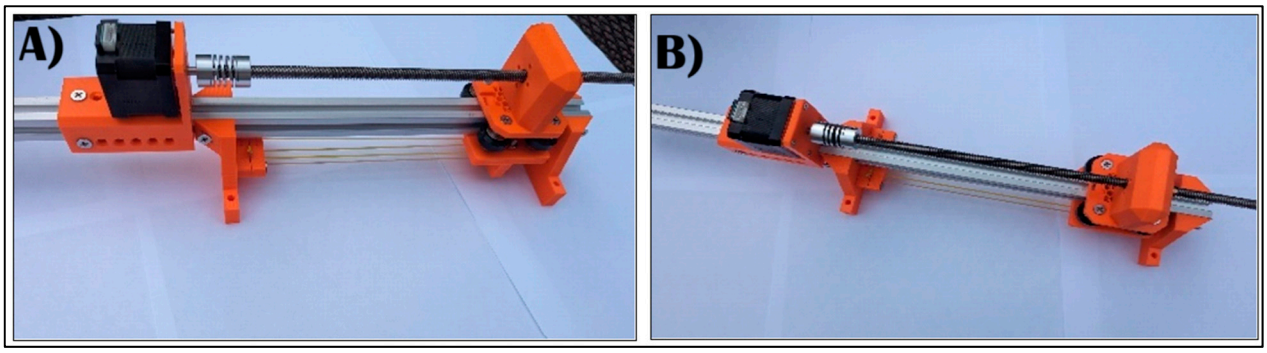

Figure 4. (**A**) Side view of the NiTi harvester prototype. (**B**) Top view of the NiTi harvester prototype.

Partially inspired by prior work, the NiTi system used torque generated by the motor, a heatsink, and NiTi wires in a self-regulating cycle. The NiTi system and its components are labeled in Figure 5.

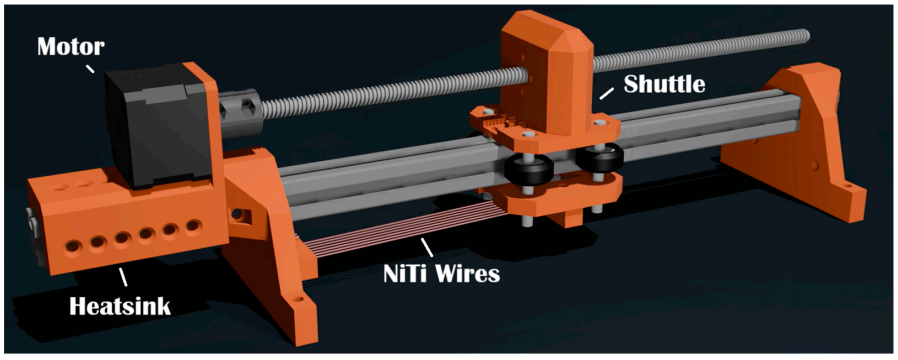

Figure 5. NiTi system with labeled components, including NiTi wires, shuttle, motor, and heatsink.

The heat caused the mechanism to self-correct by moving the wheeled shuttle toward the heatsink, cooling the active components.

As shown in Figure 6, the temperature differential and heat pump mechanism allowed the system to gather water condensate. As with the desiccant wheel, more information on its design and function is available in the Supplementary Materials.

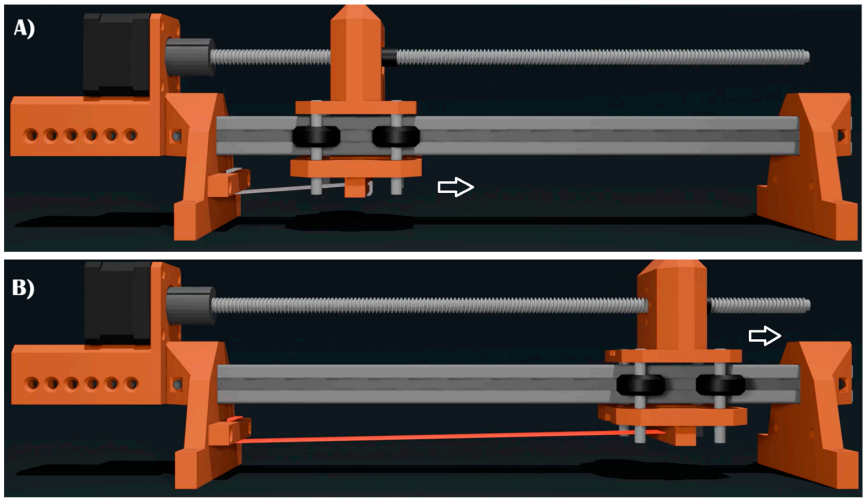

Figure 6. *Cont.*

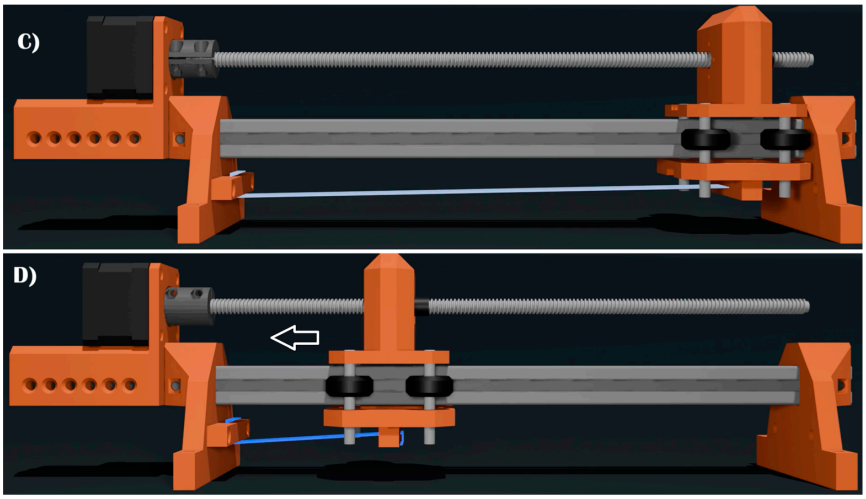

Figure 6. NiTi system cycle: (**A**) Threaded screw drives shuttle to the end of the device. (**B**) NiTi wires absorb heat while the shuttle reaches maximum extension. (**C**) NiTi wires reach thermal equilibrium with the environment. (**D**) NiTi wires are cool as the shuttle moves toward the heatsink, and water condensate is collected. The white arrow denotes the movement of the shuttle.

2.5. Testing Methodology

A testing protocol was developed and applied to evaluate the harvesters. Both the prototype and control assemblies were positioned within an enclosure equipped with a continuously operating humidifier. Readings were then systematically collected at regular 10 s intervals, with measurements such as current, temperature, and water level averaged over the time frame. Averaging measured values mitigated potential outliers and the impact of noise from the experiment. Three tests were conducted for both the control and the NiTi prototype assemblies, with the entire testing procedure performed over a cumulative duration of 30 min. Before any water was harvested, the resistive water sensor was calibrated using a controlled amount of water to ensure accuracy and precision while collecting data. Power consumption and harvesting efficiency were then calculated. A *t*-test was performed to determine differences in comparative power consumption over an average 30 min interval. Based on efficiencies reported in earlier work, we hypothesized that the elastocaloric device would achieve a higher water-harvesting rate at greater energy efficiency [2].

3. Results

3.1. Summary

The results from each harvester were combined after three trials, modeling average measurements over a 30 min interval. The temperature, power usage, and water harvesting rate were compared for the desiccant wheel and NiTi prototypes. The cumulative watt-hours were tracked and compared to other parameters. Significant differences were found between the power consumption over 30 min ($p < 0.01$).

3.2. Desiccant Wheel Design

Over a 30 min interval, the desiccant wheel harvester accumulated a total water volume of 15.67 $\pm$ 0.2 mL (Figure 7), and its average harvesting rate was 0.1567 $\pm$ 0.023 mL/WH.

With a baseline established using a traditional desiccant wheel design, the next area of interest was observing its long-term capabilities. The desiccant wheel harvester's temperature peaked at an average of 32.26 °C by the end of testing (Figure 8). The mean current used was 7.7 $\pm$ 0.14 A. At 24 V, the average highest power used by the desiccant harvester was 184.8 $\pm$ 3.36 W.

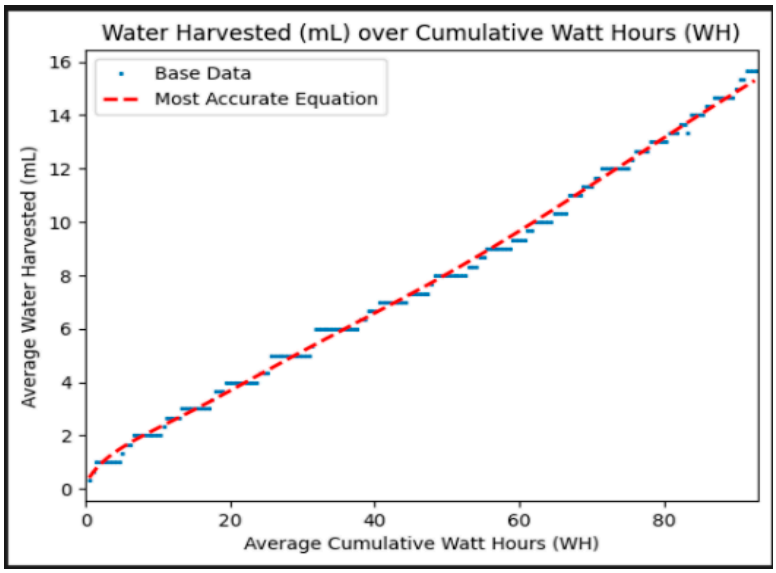

Figure 7. Tracking of the desiccant wheel water harvester over continuous water harvesting for a 30 min interval.

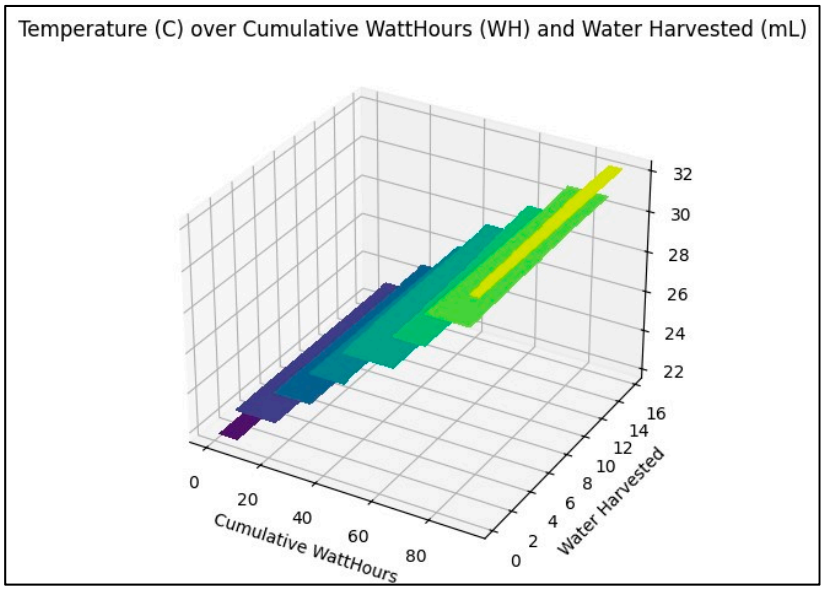

Figure 8. Temperature of desiccant wheel water harvester, tracked over continuous water harvesting for a 30 min interval. Cooler temperatures are dark blue, and warmer temperatures are yellow.

3.3. NiTi Prototype

Over a 30 min interval, the NiTi harvester collected 9.00 ± 0.1 mL of water (Figure 9). Nonetheless, the volume fluctuated slightly.

The NiTi prototype reached an average temperature of 23.38 °C with little fluctuation (Figure 10). The NiTi prototype used an average peak voltage of 23.8 V with little fluctuation range. The mean current used was 8.3 ± 0.15 A. At a power of 23.8 V, the average power used was 197.54 ± 3.57 W. The average harvesting rate with the NiTi prototype was 0.18 ± 0.027 mL/WH. However, the total watt-hours were almost half of those of the desiccant wheel design.

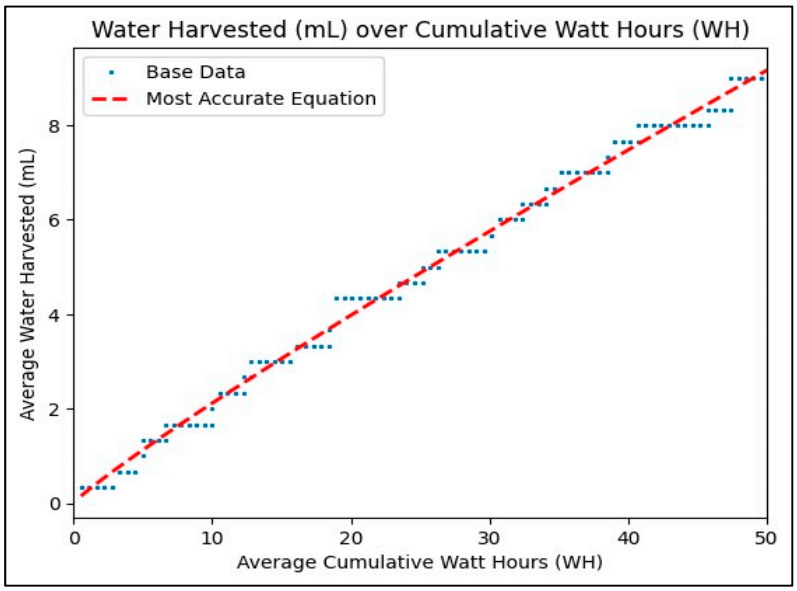

Figure 9. NiTi water harvester tracked over continuous water harvesting for a 30 min interval.

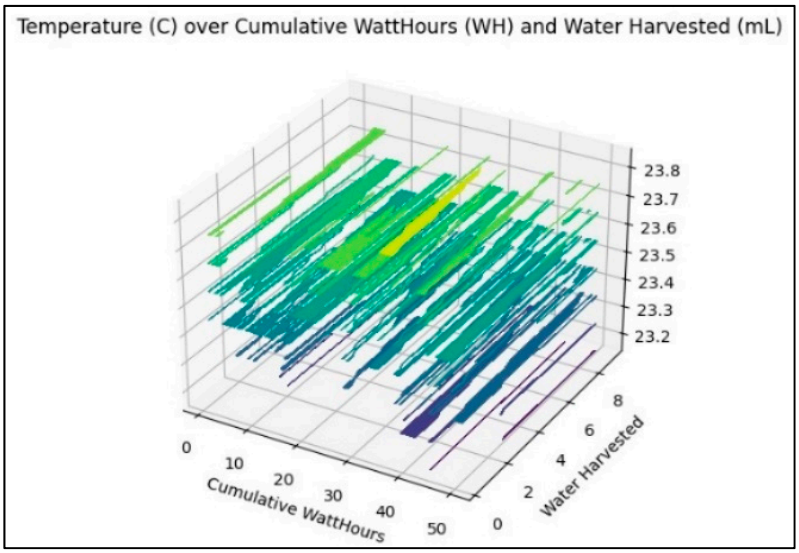

Figure 10. Temperature of the NiTi water harvester, tracked over continuous water harvesting for a 30 min interval. Cooler temperatures are dark blue, and warm temperatures are yellow.

4. Discussion

4.1. Overview

On average 30 min intervals, the NiTi harvester harvested more water (at 0.18 ± 0.027 mL/WH) than the desiccant wheel harvester (at 0.1567 ± 0.023 mL/WH). The NiTi harvester was significantly more efficient than the desiccant wheel harvester ($p < 0.01$). In addition, the desiccant wheel harvester had a wider range of temperature variation, from 22 to 32 °C. The greater power consumption and temperature increase could be attributed to the use of a heat lamp. By contrast, the average NiTi harvester temperature remained between 23 and 24 °C. While more rungs could be added to the desiccant wheel design, the device would require a more specialized temperature control [32,36]. Provided a comparable power supply, relative humidity, and enclosed volume were used for both devices, the differing outcomes can be attributed to the principles behind each device. While the NiTi harvester had only a slightly higher average AWH yield, it was designed with inbuilt thermoregulation to ensure that the system remains within a consistent temperature range.

4.2. Study Limitations

Both prototypes were based on earlier work from the literature, but many variations of each exist. Design optimization required changing parameters for each device, such as the number of rungs on the desiccant wheel. In addition, the high relative humidity (99.9%) represented an ideal circumstance rather than a realistic one. Similarly, other experimental mechanisms were excluded entirely, such as optimized air intakes and other features that are important for the system as a whole. Finally, the present methodology employed a three-trial test of 30 min each. Thus, by increasing the experimental time or the number of trials, each harvester could also be evaluated for endurance, as prior work has reported potential fatigue issues with NiTi wire [28–31]. While not substantial, a slight decrease in efficiency was noted in NiTi wires over larger fatigue cycles. Using NiTi wire bundles and tubes or adjusting the travel distance has partially been discussed in other literature [28–31].

4.3. Future Work

NiTi dehumidifiers demonstrate promising potential for AWH [33,37]. While desiccant wheel designs have been extensively explored, further research, development, and optimization of NiTi systems is required. The heat lamp was the primary reason for the high energy usage in the desiccant wheel design. While fatigue with NiTi wire remains a potential issue, thermoregulation was an advantage for this device [28–31]. Beyond AWH, NiTi dehumidifiers could be more energy-efficient options for HVAC, waste heat management in computing, firefighting in water-scarce areas, and refrigeration. Although each future application would require design refinements, the principles underlying the system were demonstrated. Ultimately, NiTi-based dehumidifiers offer advantages in yield, energy efficiency, and temperature regulation compared to conventional desiccant wheel designs [16,21].

5. Conclusions

Over a 30 min interval, the NiTi water harvester yielded an amount of water comparable to a desiccant wheel harvester at half the energy. While the energy reduction is not as outstanding as that of previous reports, this study represents a rare direct comparison of similar systems [2,33,36]. Iterative improvements are required to refine the NiTi prototype into a viable water harvester; however, its energy efficiency possesses greater potential for off-grid and portable applications. While 0.18 ± 0.027 mL/WH is not the highest value reported in a 30 min interval, it represents a favorable comparison to current technology. Mechanical design parameters for each harvester, such as a wider range of relative humidity, temperature, and airflow conditions, are required for further optimization [16,21]. In summary, elastocaloric cooling remains a significant advancement for dehumidification, making AWH more economical and feasible.

Supplementary Materials: The data, models, and supplementary information are available at: https://github.com/Multi-Volt/Flood (accessed on 13 July 204).

Author Contributions: Conceptualization, J.L. and J.S.; methodology, J.S.; software, J.S.; validation, J.L., J.S. and Q.T.; formal analysis, J.L.; investigation, J.S.; resources, Q.T.; data curation, J.L.; writing—original draft preparation, J.L. and V.V.; writing—review and editing, J.L.; visualization, J.S.; supervision, J.L. and Q.T.; project administration, J.L.; funding acquisition, Q.T. All authors have read and agreed to the published version of the manuscript.

Funding: This research received no external funding.

Institutional Review Board Statement: Not applicable.

Informed Consent Statement: Not applicable.

Data Availability Statement: The data, models, and Supplementary Information are available at: https://github.com/Multi-Volt/Flood (accessed on 13 July 2024).

Acknowledgments: The authors would like to thank The Ohio State University.

Conflicts of Interest: The authors declare no conflicts of interest.

References

1. Lopes, R.H.; Silva, C.R.D.V.; Silva, Í.D.S.; Salvador, P.T.C.D.O.; Heller, L.; Uchôa, S.A.D.C. Worldwide surveillance actions and initiatives of drinking water quality: A scoping review. *Int. J. Environ. Res. Public Health* **2022**, *20*, 559. [CrossRef] [PubMed]
2. Ge, F.; Wang, C. Exergy analysis of dehumidification systems: A comparison between the condensing dehumidification and the desiccant wheel dehumidification. *Energy Convers. Manag.* **2020**, *224*, 113343. [CrossRef]
3. Armstrong, L.E.; Johnson, E.C. Water intake, water balance, and the elusive daily water requirement. *Nutrients* **2018**, *10*, 1928. [CrossRef] [PubMed]
4. Braun, H.; von Andrian-Werburg, J.; Malisova, O.; Athanasatou, A.; Kapsokefalou, M.; Ortega, J.; Mora-Rodriguez, R.; Thevis, M. Differing water intake and hydration status in three European countries—A day-to-day analysis. *Nutrients* **2019**, *11*, 773. [CrossRef] [PubMed]
5. Nakamura, Y.; Watanabe, H.; Tanaka, A.; Yasui, M.; Nishihira, J.; Murayama, N. Effect of increased daily water intake and hydration on health in Japanese adults. *Nutrients* **2020**, *12*, 1191. [CrossRef] [PubMed]
6. Raymond, C.; Matthews, T.; Horton, R.M. The emergence of heat and humidity too severe for human tolerance. *Sci. Adv.* **2020**, *6*, eaaw1838. [CrossRef] [PubMed]
7. Slekiene, J.; Mosler, H.J. The link between mental health and safe drinking water behaviors in a vulnerable population in rural Malawi. *BMC Psychol.* **2019**, *7*, 44. [CrossRef]
8. Matthews, T. Humid heat and climate change. *Prog. Phys. Geogr. Earth Environ.* **2018**, *42*, 391–405. [CrossRef]
9. Zhuang, J.; Payyappalli, V.M.; Behrendt, A.; Lukasiewicz, K. *Total Cost of Fire in the United States*; Fire Protection Research Foundation: Buffalo, NY, USA, 2017.
10. Liao, Y.; Kousky, C. The fiscal impacts of wildfires on California municipalities. *J. Assoc. Environ. Resour. Econ.* **2022**, *9*, 455–493. [CrossRef]
11. Struzik, E. How Wildfires Are Polluting Rivers and Threatening Water Supplies. YaleEnvironment360. 2 October 2018. Available online: https://e360.yale.edu/features/how-wildfires-are-polluting-rivers-and-threatening-water-supplies (accessed on 18 February 2024).
12. Meng, Y.; Dang, Y.; Suib, S.L. Materials and devices for atmospheric water harvesting. *Cell Rep. Phys. Sci.* **2022**, *3*, 100976. [CrossRef]
13. Gao, Y.; Wang, J.; Xia, W.; Mou, X.; Cai, Z. Reusable Hydrophilic–superhydrophobic patterned weft backed woven fabric for high-efficiency water-harvesting application. *ACS Sustain. Chem. Eng.* **2018**, *6*, 7216–7220. [CrossRef]
14. Huang, Z.X.; Liu, X.; Wong, S.C.; Qu, J.P. A single step fabrication of bio-inspired high efficiency and durable water harvester made of polymer membranes. *Polymer* **2019**, *183*, 121843. [CrossRef]
15. Xiang, C.; Yang, X.; Deng, F.; Chen, Z.; Wang, R. Daytime air–water harvesting based on super hygroscopic porous gels with simultaneous adsorption–desorption. *Appl. Phys. Rev.* **2023**, *10*, 041413. [CrossRef]
16. Lu, Z.; Fix, A.J.; Warsinger, D.M.; Braun, J.E.; Ziviani, D. Generalization of second law efficiency for next-generation cooling and dehumidification systems. *Energy Convers. Manag.* **2024**, *300*, 117972. [CrossRef]
17. Kushwaha, P.K.; Kumar, A.; Choudhary, R. Solar-powered water generation from atmospheric air using desiccant wheel: Theoretical and experimental investigation. *Sol. Energy Mater. Sol. Cells* **2024**, *274*, 112969. [CrossRef]
18. Li, J.; Xing, G.; Qiao, M.; Du, S.; Zhou, T.; Gao, S.; Sun, H.; Jiao, R.; Li, A. Composite porous 3D foam for solar-driven atmospheric water harvesting in low humidity natural environment. *Chem. Eng. J.* **2024**, *490*, 151543. [CrossRef]
19. Shan, H.; Pan, Q.; Xiang, C.; Poredoš, P.; Ma, Q.; Ye, Z.; Hou, G.; Wang, R. High-yield solar-driven atmospheric water harvesting with ultra-high salt content composites encapsulated in porous membrane. *Cell Rep. Phys. Sci.* **2021**, *2*, 100664. [CrossRef]
20. Su, M.; Han, X.; Chong, D.; Wang, J.; Liu, J.; Yan, J. Experimental study on the performance of an improved dehumidification system integrated with precooling and recirculated regenerative rotary desiccant wheel. *Appl. Therm. Eng.* **2021**, *199*, 117608. [CrossRef]
21. Zhang, Q.; Li, Y.; Zhang, Q.; Ma, F.; Lü, X. Application of deep dehumidification technology in low-humidity industry: A review. *Renew. Sustain. Energy Rev.* **2024**, *193*, 114278. [CrossRef]
22. Cui, J.; Seelecke, S.; Motzki, P.; Sun, Q.; Takeuchi, I. Prototype Progress Report: Elastocaloric Heat Pumps. *AM&P Tech. Artic.* **2024**, *182*, 49–52.
23. Wang, Y.; Liu, Y.; Xu, S.; Zhou, G.; Yu, J.; Qian, S. Towards practical elastocaloric cooling. *Commun. Eng.* **2023**, *2*, 79. [CrossRef]
24. Liu, B.; Wang, Y.; Zhu, Z.; Theodorakis, P.E.; Song, J.; Bennacer, R. A lower temperature difference of the elastocaloric effect by natural rubber. *Int. J. Refrig.* **2023**, *155*, 163–172. [CrossRef]
25. Dykstra, D.M.; Lenting, C.; Masurier, A.; Coulais, C. Buckling metamaterials for extreme vibration damping. *Adv. Mater.* **2023**, *35*, 2301747. [CrossRef] [PubMed]
26. Xu, J.; Bruederlin, F.; Bumke, L.; Ossmer, H.; Quandt, E.; Miyazaki, S.; Kohl, M. SMA Film-Based Elastocaloric Cooling Devices. *Shape Mem. Superelasticity* **2024**, *10*, 119–133. [CrossRef]
27. Cheng, S.; Li, Z.; Lee, W.Z.; Liu, S.; Fu, Y.; Zhao, Y.; Zhang, M. Development of a crankshaft driven single long NiTi tube compressive elastocaloric cooler. *Sci. Technol. Built Environ.* **2023**, *29*, 809–822. [CrossRef]

28. Cui, J.; Wu, Y.; Muehlbauer, J.; Hwang, Y.; Radermacher, R.; Fackler, S.; Wuttig, M.; Takeuchi, I. Demonstration of high efficiency elastocaloric cooling with large ΔT using NiTi wires. *Appl. Phys. Lett.* **2012**, *101*, 073904. [CrossRef]
29. Welsch, F.; Kirsch, S.; Louia, F.; Seelecke, S.; Motzki, P. Investigation of the thermal heat exchange between NiTi-wire bundles and airflow for different wire arrangements. In Proceedings of the ASME 2023 Conference on Smart Materials, Adaptive Structures and Intelligent Systems, Austin, TX, USA, 11–13 September 2023; Volume 87523, p. V001T04A023.
30. Cheng, S. Modelling a Single Long NiTi Tube Compressive Elastocaloric Cooler Using Lumped Analysis Method. 31 July 2023. Available online: http://dx.doi.org/10.2139/ssrn.4527433 (accessed on 2 July 2024).
31. Liang, D.; Wang, Q.; Chu, K.; Chen, J.; Hua, P.; Ren, F.; Sun, Q. Ultrahigh cycle fatigue of nanocrystalline NiTi tubes for elastocaloric cooling. *Appl. Mater. Today* **2022**, *26*, 101377. [CrossRef]
32. Li, X.; Hua, P.; Sun, Q. Continuous and efficient elastocaloric air cooling by coil-bending. *Nat. Commun.* **2023**, *14*, 7982. [CrossRef]
33. Qian, S.; Catalini, D.; Muehlbauer, J.; Liu, B.; Mevada, H.; Hou, H.; Hwang, Y.; Radermacher, R.; Takeuchi, I. High-performance multimode elastocaloric cooling system. *Science* **2023**, *380*, 722–727. [CrossRef]
34. Cheng, S. Design of a Large-Power Separated Long NiTi Tube Bundle Compressive Elastocaloric Cooler. 31 August 2023. Available online: http://dx.doi.org/10.2139/ssrn.4558662 (accessed on 2 July 2024).
35. Xiao, L.; Chi, J.; Luo, K.; Xu, J.; Zhao, D.; Wu, Z.; Luo, E. A highly efficient eco-friendly heat-driven thermoacoustic refrigerator using nitrogen and water. *Energy Convers. Manag.* **2024**, *304*, 118251. [CrossRef]
36. Cirillo, L.; Greco, A.; Masselli, C. The energy performances of an elastocaloric device for air conditioning through numerical investigation. *Appl. Therm. Eng.* **2024**, *236*, 121517. [CrossRef]
37. Wang, B.; Zhou, X.; Guo, Z.; Liu, W. Recent advances in atmosphere water harvesting: Design principle, materials, devices, and applications. *Nano Today* **2021**, *40*, 101283. [CrossRef]
38. Tsujiguchi, T.; Osaka, Y.; Kodama, A. Study on the miniaturization of the desiccant wheel by the optimization of designing/operation concept. *J. Chem. Eng. Jpn.* **2024**, *47*, 608–614. [CrossRef]